Original Article

Cobalt Zinc Ferrite Nanoparticles as a Potential Magnetic Resonance Imaging Agent: An *In vitro* Study

Zeinab Ghasemian [1], Daryoush Shahbazi-Gahrouei [1*], and Sohrab Manouchehri [2]

1. Department of Medical Physics, School of Medicine, Isfahan University of Medical Sciences, Isfahan, Iran
2. Department of Physics, Nano-center, Maleke-ashtar University of Technology, Shahin-shahr, Isfahan, Iran

*** Corresponding author:**
Daryoush Shahbazi-Gahrouei, Ph.D., Department of Medical Physics, Faculty of Medicine, Isfahan University of Medical Sciences, Isfahan, Iran
Tel: +98 31 37922495
Fax: +98 31 37922432
E-mail:
shahbazi24@yahoo.com &
shahbazi@med.mui.ac.ir
Received: 11 Oct 2014
Accepted: 23 Dec 2014

Abstract

Background: Magnetic Nanoparticles (MNP) have been used for contrast enhancement in Magnetic Resonance Imaging (MRI). In recent years, research on the use of ferrite nanoparticles in T_2 contrast agents has shown a great potential application in MR imaging. In this work, $Co_{0.5}Zn_{0.5}Fe_2O_4$ and $Co_{0.5}Zn_{0.5}Fe_2O_4$-DMSA magnetic nanoparticles, CZF-MNPs and CZF-MNPs-DMSA, were investigated as MR imaging contrast agents.

Methods: Cobalt zinc ferrite nanoparticles and their suitable coating, DMSA, were investigated under *in vitro* condition. Human prostate cancer cell lines (DU145 and PC3) with bare (uncoated) and coated magnetic nanoparticles were investigated as nano-contrast MR imaging agents.

Results: Using T_2-weighted MR images identified that signal intensity of bare and coated MNPs was enhanced with increasing concentration of MNPs in water. The values of $1/T_2$ relaxivity (r_2) for bare and coated MNPs were found to be 88.46 and 28.80 (mM^{-1} s^{-1}), respectively.

Conclusion: The results show that bare and coated MNPs are suitable as T_2-weighted MR imaging contrast agents. Also, the obtained r_2/r_1 values (59.3 and 50) for bare and coated MNPs were in agreement with the results of other previous relevant works.

Avicenna J Med Biotech 2015; 7(2): 64-68

Keywords: Magnetite Nanoparticles, MR imaging, Prostatic neoplasm

Introduction

One of the most powerful non-invasive techniques for diagnosis is MR imaging which has excellent temporal and spatial (25-100 μm) resolution [1-3]. The limitation of MR imaging technique is its low sensitivity that leads to unclear diagnosis of healthy tissues from abnormal tissues. Theoretically, the sensitivity in MR imaging is due to the relaxivity of magnetic spins in water protons [4]. In the last decades, nanoparticle agents continue to receive considerable attention in the field of medical imaging as potential MR imaging contrast agents [5,6]. Recently, magnetic nanoparticles have attracted growing interest as high performance biomaterials which are used for the diagnosis and treatment of cancers. Nowadays, more studies focus on magnetic nanoparticles as potential MR imaging contrast agents. Magnetic nanoparticles should have features such as uniform particle size [6], a uniform and high superparamagnetic moment, high colloidal stability, low toxicity and high biocompatibility [7]. Magnetic nanoparticles can alter longitudinal and transverse relaxation times and thereby affect the MR image signal [8]. Studies on the application of ferrite nanoparticles in T_2 MR imaging contrast agents has shown great potential [5,9-11].

Saturation magnetization (Ms) value is one of the most dominant parameters that affect T_2 relaxivity [12]. Jun *et al* reported that the values of Ms are dependent on the size and composition of nanoparticles [13]. Metallic nanoparticles such as iron, nickel, cobalt, or their alloys have higher magnetization value than that of oxide nanoparticles [14]. For this reason, in this study, cobalt zinc ferrite ($Co_{0.5}Zn_{0.5}Fe_2O_4$) magnetic nanoparticles were used for further investigation.

In another study, Barcena *et al* found that zinc ferrite nanoparticles increased the $1/T_2$ relaxivity and improved the sensitivity of detection by MR imaging [3]. In previous studies, special attention was given to particles coated with Dimercaptosuccinic acid (DMSA) for biomedical applications [15-17]. Recently, the cytotoxicity effect of DMSA-Fe_2O_3 by tetrazolium dye assay on human aortic endothelial cells was reported which revealed its low cytotoxicity effect [15]. Also, the cytotoxicity of CZF-MNPs and CZF-MNPs-DMSA was also demonstrated on prostate cancer cells (PC3 and DU145) [18].

The aim of this paper was to evaluate the influence of coated and uncoated magnetic nanoparticles, in par-

ticular CZF-MNPs and CZF-MNPs-DMSA, on the relaxivity of water protons as MR imaging contrast agent or molecular imaging for clinical diagnosis.

Materials and Methods

Preparation and synthesis, characterization, coating with DMSA, and cytotoxicity of cobalt zinc ferrite nanoparticles were described in previous published papers [16,18]. Briefly, cobalt zinc ferrite nanoparticles were prepared using a co-precipitation method and their characterization was assessed using of TEM (Transmission Electron Microscopy), FT-IR (Furier Transformation Infrared Spectroscopy) and magnetization measurements.

Cell culture

Human prostate cancer cells, HPCs, (DU145 and PC3) were purchased from the National Cell Bank of Iran, Pasteur Institute of Iran. They were cultured in Roswell Park Memorial Institute (RPMI) media supplemented with 1% antibiotics (100 *units/ml* penicillin and 100 *µg/ml* streptomycin) and 10% Fetal Bovine Serum (FBS) until the third passage before performing the experiments. All the cell culture materials were from Gibco, USA. Cells were grown to confluence at 37°*C* in 5% CO_2/air. *In vitro* cytotoxicity (MTT assay) of coated and bare magnetic nanoparticles was evaluated using standard 3-(4, 5-dimethylthiazol-2yl)-2, 5-diphenyltetrazolium bromide (MTT) based colorimetric assay as described elsewhere [18]. The cell viability was determined by the following formula:

$$\%\ \text{Cell viability} = \frac{\text{Mean absorbance in test wells}}{\text{Mean absorbance in control}} \times 100$$

Incubation of cells with the bare and coated MNPs

First, gelatin suspension 1 *g* was prepared from powder gelatin dissolved in 50 *ml* PBS solution, and put in water bath for 30 *min* to obtain uniform solution. Two prostate cancer cell lines (PC3 and DU145) were incubated with different concentrations (0.5, 1 and 1.5 *mmol*) of CZF-MNPs and CZF-MNPs-DMSA for 2 *hr* at room temperature in RPMI 1640 culture medium. In order to separate the particles stuck together, before adding bare and coated MNPs suspension with different concentrations into RPMI culture medium, they were sonicated for 20 *min*. Then, the cells were washed three times with PBS solution. In the next step, 1 *ml* of gelatin suspension was added to 1.5 *ml* Eppendorf tubes with different concentrations and stirred to obtain uniform solution. Then, the Eppendorf tubes with different concentrations were placed on ice powder until solidity was obtained in the solution. Control groups received only 1 *ml* of gelatin suspension.

In vitro MR imaging

These Eppendorf tubes with different concentrations were used for *in vitro* MR imaging characterizations. T_2-weighted images were obtained using a 1.5T MRI scanner (1.5 Tesla, GE Medical system).

Relaxivity (r_1 and r_2) measurements

For MR imaging studies, different concentrations of coated and bare MNPs were prepared in 1.5 *ml* Eppendorf tubes. The longitudinal and transverse relaxation times (T_1 and T_2) were measured using 3 Tesla field strength (Siemens MR scanner with head coil). MR images of each sample were obtained using a standard spin-echo sequence with two following parameters:
Repetition time (T_R)=4000 *ms*, echo time (T_E)=12, 24, 36, 48, 60 and 72 *ms*, number of echoes (NE)=6, matrix size=512×384, pixel band width=230, slice thickness=2.5 *mm*, number of excitations (NEX)=3 and field of view=25 *cm*.
Repetition time (T_R)=100, 250, 500, 1000, 2000 and 4000 *ms*, echo time (T_E)=15 *ms*, number of excitations (NEX)=3, matrix size=512×384, pixel band width=130, slice thickness=2.5 *mm*, number of echoes (NE)=1 and field of view=25 *cm*.

Results

The surface morphology of CZF-MNPs and CZF-MNPs-DMSA was evaluated by TEM and their results are shown in previous publications [18]. The findings showed that particles had almost spherical structures. Indeed, the average particle sizes of CZF-MNPs and CZF-MNPs-DMSA (co-precipitation) were 16 and 40 *nm*, respectively.

In vitro MR imaging

The capability and suitability of synthesized nanoparticles as MR contrast agent was confirmed using a T_2-weighted image protocol by 1.5 Tesla (GE Medical system) MR imaging system. The results are shown in figure 1. This result demonstrated that both bare and coated nanoparticles have been imported in PC3 and DU145 cell lines and resulted in grating signal intensity reduction.

The T_2-weighted MR image in figure 1 also shows that CZF-MNPs and CZF-MNPs-DMSA induce a negative contrast. In addition, for the same Fe content, the enhancement in intensity using CZF-MNPs is the same as the amount of CZF-MNPs-DMSA.

Relaxivity (r_1 and r_2) measurements

Figure 2 shows T_2-weighted MR images of different concentrations of bare and coated MNPs (CZF-MNPs and CZF-MNPs-DMSA) by 3 Tesla, MR imaging system with standard spin-echo sequence (T_R=1000 *ms*, T_E=12 *ms*, room temperature). As can be seen from this figure, significant differences are observed between signal intensity at different concentrations of bare and

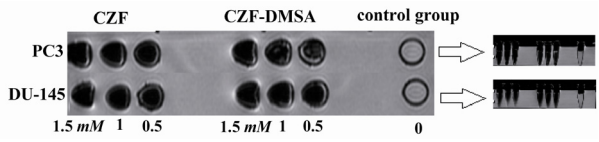

Figure 1. T_2-weighted magnetic resonance images at various Fe concentrations, CZF-MNPs and CZF-MNPs-DMSA (1.5 T, Fast spin-echo sequence: T_R=2520 *ms*, T_E=102 *ms*, room temperature).

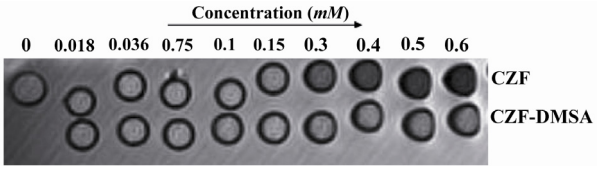

Figure 2. MR imaging signal intensity of bare and coated MNPs for different concentrations of Fe (*mM*) using 3 T, standard spin-echo sequence: T_R=1000 *ms*, T_E=12 *ms*, room temperature).

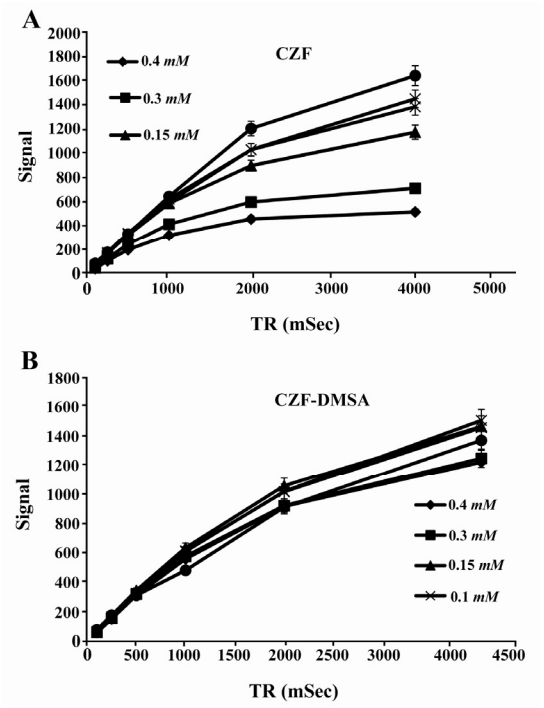

Figure 3. Plots of signal intensity for (A) CZF-MNPs and (B) CZF-MNPs-DMSA as a function of T_R for different Fe concentrations (*mM*) of bare and coated MNPs. The signal intensity for each sample was measured three times.

coated nanoparticles. Also, the reduction of signal intensity in CZF-MNPs sample is more than that of CZF-MNPs-DMSA sample (in the same concentration). In addition, the signal intensity of CZF-MNPs was enhanced by decreasing CZF-MNPs concentrations in water solution. Two samples were prepared in dark state in the MR image where the composites (contrast agents) were collected.

Relaxivity ratio (r_2/r_1) is an important index to determine the ability of nanoparticles as T_2 MR imaging contrast agent. T_1 and T_2 relaxivity values, size (*nm*), saturation magnetization (Ms) and r_2/r_1 values of CZF-MNPs and CZF-MNPs-DMSA are presented in table 1. Plots of signal intensity for CZF-MNPs and CZF-MNPs- DMSA as a function of T_R and T_E for different

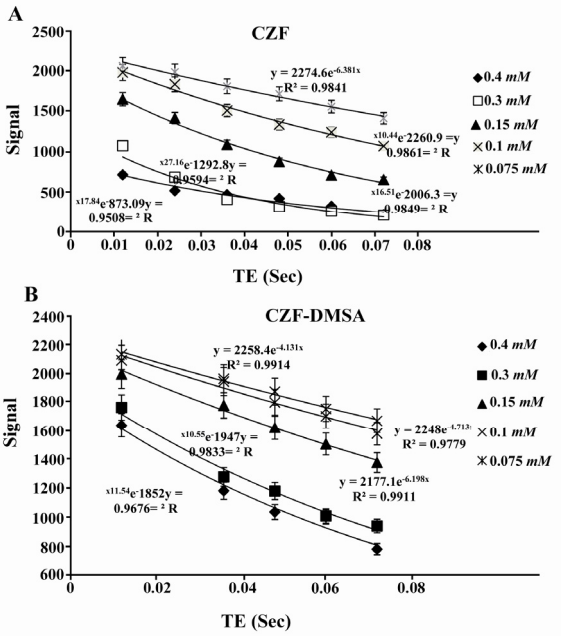

Figure 4. Plots of signal intensity for (A) CZF-MNPs and (B) CZF-MNPs-DMSA as a function of T_E for different Fe concentrations (*mM*) of bare and coated MNPs.

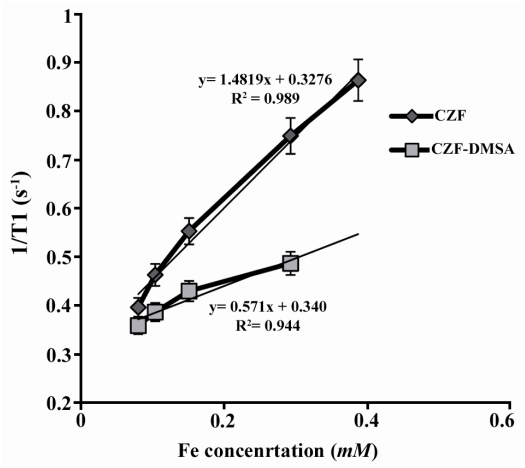

Figure 5. Plot of longitudinal relaxivity ($1/T_1$) for CZF-MNPs and CZF-MNPs-DMSA as a function of different Fe concentrations (*mM*).

Fe (*mM*) concentrations of bare and coated MNPs was measured three times and their results are shown in figures 3 and 4, respectively. Two $1/T_2$ and $1/T_1$ relaxivity values of samples have been calculated and are presented in figures 5 and 6.

R_2 values of relaxation rates (r_1 and r_2) were higher than 0.9, which indicated a good fitness for regression due to high values of r_2/r_1 for bare and coated MNPs. These two magnetic nanoparticles are classified as

Table 1. Relaxivities r_1 and r_2 (at 3 T), size and saturation magnetization (Ms) of bare and coated MNPs

MNPs formulation	Size (*nm*)	Saturation magnetization (Ms) (*emu/g*)	r_1(mM^{-1} s^{-1})	R^$_2$ value	r_2(mM^{-1} s^{-1})	R^$_2$ value	r_2/r_1
CZFMNPs (co-precipitation)	16	43.1	1.490	0.987	88.46	0.972	59.3
CZF-MNPs@DMSA (co-precipitation)	40	42.4	0.577	0.940	28.80	0.999	50.0

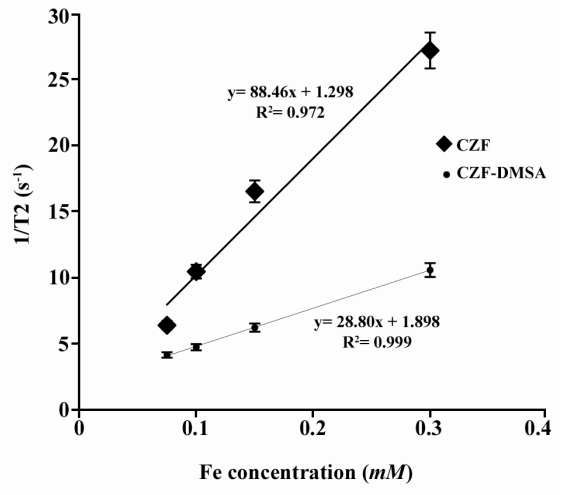

Figure 6. Plot of transverse relaxivity R_2 ($1/T_2$) for CZF-MNPs and CZF-MNPs-DMSA as a function of different Fe concentrations (*mM*).

negative MR imaging contrast agents.

The lower graphs in figures 5 and 6 are related to r_1 and r_2 for coated MNPs which were compared to the bare MNPs. In other words, the relaxation curves for bare MNPs are steeper than that of the coated MNPs, either longitudinal or transverse relaxivity.

Discussion

The ability of both CZF and CZF-DMSA nanoparticles was assessed in order to decrease the longitudinal (T_1) and transverse (T_2) relaxation times of water protons. The MR imaging study showed that both T_1 and T_2 relaxation times were reduced with increasing Fe (*mM*) concentration; hence, CZF-MNPs and CZF-MNPs-DMSA may be more favorable as negative MR imaging contrast agents. The transverse and longitudinal relaxivity (r_1 and r_2) of water protons were increased by increasing Fe (*mM*) concentration of bare and coated MNPs compared to the control group (gelatin suspension).

The values of the saturation magnetization of bare and coated nanoparticles were approximately the same and found to be 43.1 and 44.4, respectively. But, regarding r_2 relaxivity of both studied magnetic nanoparticles, bare nanoparticle (CZF-MNPs) has r_2 of 3-fold higher than that of coated nanoparticle (CZF-MNPs-DMSA). Although the saturation magnetization of both bare and coated MNPs was so similar but many differences between r_2 relaxivitiies of two studied samples was observed. Therefore, the other factors such as particle size and shape of nanoparticles influence the relaxation time.

According to literature, factors such as synthesis method of nanoparticles and the type of their coating can affect both T_1 and T_2 relaxation times [9]. The study of Hoque *et al* showed that synthesized nanoparticles using sonochemical technique has r_2 relaxivity values higher than that of co-precipitation technique [10]. Findings of this study showed that r_2/r_1 values for CZF-MNPs and CZF-MNPs-DMSA turned out to be 59.3 and 50, respectively. MR imaging results also showed that transverse and longitudinal relaxivities were increased with increasing Fe (*mM*) concentration. For this reason, our findings showed that CZF-MNPs and CZF-MNPs-DMSA are desirable negative nano contrast MR imaging agents.

Conclusion

The values of r_2 relaxivity and r_2/r_1 ratio showed that bare and coated MNPs may be suitable T_2 contrast agents. But, the low values of r_1 relaxivity, and also the low values of r_2/r_1 ratio indicated that bare and coated MNPs are not acceptable T_1 MR imaging nano-contrast agents. Further study should be done to evaluate whether cobalt zinc ferrite nanoparticles with different coatings can be used as T_2 MR imaging contrast agents. In addition, this magnetic nanoparticle should be synthesized with other methods and be coated with other different suitable materials.

Acknowledgement

This work was supported by Isfahan University of Medical Science (IUMS).

Conflict of Interest

None declared.

References

1. Massoud TF, Gambhir SS. Molecular imaging in living subjects: seeing fundamental biological processes in a new light. Genes Dev 2003;17(5):545-580.
2. Shahbazi-Gahrouei D, Williams M, Rizvi S, Allen BJ. In vivo studies of Gd-DTPA-monoclonal antibody and gd-porphyrins: potential magnetic resonance imaging contrast agents for melanoma. J Magn Reson Imaging 2001; 14(2):169-174.
3. Corti M, Lascialfari A, Micotti E, Castellano A, Donativi M, Quarta A, et al. Magnetic properties of novel superparamagnetic MRI contrast agents based on colloidal nanocrystals. J Magn Magn Mater 2008;320(14):e320-e323.
4. Abdolahi M, Shahbazi-Gahrouei D, Laurent S, Sermeus C, Firozian F, Allen BJ, et al. Synthesis and in vitro evaluation of MR molecular imaging probes using J591 mAb-conjugated SPIONs for specific detection of prostate cancer. Contrast Media Mol Imaging 2013;8(2):175-184.
5. Shahbazi-Gahrouei D, Abdolahi M. Superparamagnetic iron oxide-C595: Potential MR imaging contrast agents for ovarian cancer detection. J Med Phys 2013;38(4): 198-204.
6. Laurent S, Forge D, Port M, Roch A, Robic C, Vander Elst L, et al. Magnetic iron oxide nanoparticles: synthesis, stabilization, vectorization, physicochemical charac-

terizations, and biological applications. Chem Rev 2008; 108(6):2064-2110.

7. Zeng C, Shi X, Wu B, Zhang D, Zhang W. Colloids containing gadolinium-capped gold nanoparticles as high relaxivity dual-modality contrast agents for CT and MRI. Colloids Surf B Biointerfaces 2014;123:130-135.
8. Shahbazi-Gahrouei D, Abdolahi M. Detection of MUC1-expressing ovarian cancer by C595 monoclonal antibody-conjugated SPIONs using MR imaging. Scientific World Journal 2013;2013:609151.
9. Barcena C, Sra AK, Chaubey GS, Khemtong C, Liu JP, Gao J. Zinc ferrite nanoparticles as MRI contrast agents. Chem Commun (Camb) 2008;(19):2224-2226.
10. Hoque SM, Srivastava C, Srivastava N, Venkateshan N, Chattopadhyay K. Synthesis and characterization of Fe- and Co-based ferrite nanoparticles and study of the T1 and T2 relaxivity of chitosan-coated particles. J Mater Sci 2013;48(2):812-818.
11. Arsalani N, Fattahi H, Nazarpoor M. Synthesis and characterization of PVP-functionalized superparamagnetic Fe3O4 nanoparticles as an MRI contrast agent. Exp Polym Lett 2010;4(6):329-338.
12. Tong S, Hou S, Zheng Z, Zhou J, Bao G. Coating optimization of superparamagnetic iron oxide nanoparticles for high T2 relaxivity. Nano Lett 2010;10(11):4607-4613.
13. Jun YW, Huh YM, Choi JS, Lee JH, Song HT, Kim S, et al. Nanoscale size effect of magnetic nanocrystals and their utilization for cancer diagnosis via magnetic resonance imaging. J Am Chem Soc 2005;127(16):5732-5733.
14. Seo WS, Lee JH, Sun X, Suzuki Y, Mann D, Liu Z, et al. FeCo/graphitic-shell nanocrystals as advanced magnetic-resonance-imaging and near-infrared agents. Nat Mater 2006;5(12):971-976.
15. Ge G, Wu H, Xiong F, Zhang Y, Guo Z, Bian Z, et al. The cytotoxicity evaluation of magnetic iron oxide nanoparticles on human aortic endothelial cells. Nanoscale Res Lett 2013;8(1):215.
16. Manouchehri S, Ghasemian Z, Shahbazi-Gahrouei D, Abdolahi M. Synthesis and characterization of cobalt-zinc ferrite nanoparticles coated with DMSA. Chem Xpress 2013;2(3):147-152.
17. Cabrera LI, Somoza A, Marco JF, Serna CJ, Morales MP. Synthesis and surface modification of uniform MFe2O4 (M=Fe, Mn, and Co) nanoparticles with tunable sizes and functionalities. J Nanopar Res 2012;14(6):1-14.
18. Shahbazi-Gahrouei D, Ghasemian Z, Abdolahi M, Manouchehri S, Javanmard SH, Dana N. In vitro evaluation of cobalt-zinc ferrite nanoparticles coated with DMSA on human prostate cancer cells. J Mol Biomark Diagn 2013; 4(3):154.